


# High-Aspect-Ratio Grating Microfabrication by Platinum- Assisted Chemical Etching and Gold Electroplating

**Journal Article****Author(s):**

Romano, Lucia ; Vila-Comamala, Joan; Jefimovs, Konstantins; Stampanoni, Marco

**Publication date:**

2020-10

**Permanent link:**

<https://doi.org/10.3929/ethz-b-000421069>

**Rights / license:**

[In Copyright - Non-Commercial Use Permitted](#)

**Originally published in:**

Advanced Engineering Materials 22(10), <https://doi.org/10.1002/adem.202000258>

**Funding acknowledgement:**

183568 - GI-BCT - Clinical Grating Interferometry Breast Computed Tomography (SNF)  
727246 - Metal Assisted chemical etching of Gratings for x-ray InterferometriC systems (EC)

**High aspect ratio grating microfabrication by Pt assisted chemical etching and Au electroplating**

*Lucia Romano\*, Joan Vila-Comamala, Konstantins Jefimovs, Marco Stampanoni*

Dr. L. Romano, Dr. J. Vila-Comamala, Dr. K. Jefimovs, Prof. M. Stampanoni  
Paul Scherrer Institut, Forschungsstrasse 111, CH-5232 Villigen, Switzerland  
Institute for Biomedical Engineering, University and ETH Zürich, 8092 Zürich, Switzerland  
E-mail: lucia.romano@psi.ch

Dr. L. Romano  
Department of Physics and CNR-IMM- University of Catania, 64 via S. Sofia, 95123 Catania,  
Italy

Keywords: metal assisted chemical etching, X-ray optics, silicon, X-ray imaging

Diffraction optics play a key role in hard X-rays imaging for which many scientific, technological and biomedical applications exist. Herein, high aspect ratio microfabrication of gratings for X-ray interferometry is demonstrated by using Pt as catalyst for metal assisted chemical etching of Si in a solution of HF and H<sub>2</sub>O<sub>2</sub>. The Pt layer has been thermally treated in order to realize a porous catalyst layer that stabilizes the etching of pattern with a pitch size from 4.8 to 20 μm in the direction perpendicular to the <100> Si substrate and an aspect ratio up to 60:1. The superior etching performance of Pt as catalyst and its stability in a solution with high HF content have been reported in direct comparison with Au catalyst for the same grating parameters. The Si structure is then used as a template for filling with Au, as a high absorbing X-ray material. The Pt catalyst layer was used as a conductive seed for Au electroplating. The quality of the overall process has been assessed by obtaining the visibility map using 30 μm thick Au grating in a X-ray interferometric set-up at 20 keV.

## 1. Introduction

Submitted version (High aspect ratio grating microfabrication by Pt assisted chemical etching and Au electroplating, by L. Romano, J. Vila-Comamala, K. Jefimovs and M. Stampanoni, Advanced Engineering Materials, Copyright © 2020, Advanced Engineering Materials, Wiley-VCH Verlag GmbH & Co. KGaA) <https://doi.org/10.1002/adem.202000258>

Metal-assisted chemical etching (MacEtch) has been deeply investigated for several purposes with the final goal of assessing a new fabrication technology that has the huge potential to overcome the limitations in aspect ratio and cost of plasma etching. Since its discovery in 2000 by Li et al.<sup>[1]</sup> MacEtch of silicon has emerged as a new technique capable of fabricating 3D nano- and micro-structures of several shapes and applications – nanoporous film, nanowires, 3D objects, trenches, vias, sensor devices, X-ray optics – in few semiconductors substrates – Si, Ge, poly-Si, GaAs etc <sup>[2, 3]</sup> –and different catalyst – Ag, Au, Cu, Pt, Pd <sup>[2]</sup>. In a typical MacEtch, the metal patterned Si substrate is immersed in a solution of HF and H<sub>2</sub>O<sub>2</sub>. The metal serves as a catalyst for H<sub>2</sub>O<sub>2</sub> reduction with a consequent holes injection deep into the valence band of the Si substrate.<sup>[1]</sup> The concentration of holes becomes higher in the region of Si surrounding the metal catalyst, silicon is there readily oxidized by HF to form silicon fluoride compounds with the reaction continuing as the catalyst is pulled into the substrate. There are very few data in literature about the use of platinum as MacEtch catalyst, it has been mostly investigated in a form of nanoparticles<sup>[4, 5]</sup> or added as top layer of Au thick film.<sup>[6]</sup> Platinum has been recently investigated as alternative MacEtch catalyst for high aspect ratio structures due to its superior catalytic activity and its stability on Si surface due to the formation of stable silicide compounds.<sup>[7]</sup> In this paper, we investigate the possibility of using Pt in wet-MacEtch to fabricate high aspect ratio gratings for X-ray interferometry. Platinum metal de-wetting has been implemented to improve the catalyst stability for micropatterns and the etching performances of MacEtch. Main steps of a full microfabrication procedure are sketched in **Figure 1**: a) growth of native silicon oxide on Si substrate; b) pattern definition by means of a lithographic process; c) Pt deposition by evaporation; d) lift-off; e) Pt de-wetting by thermal treatment; f) MacEtch in a solution of HF and H<sub>2</sub>O<sub>2</sub>; g) Si side wall

oxidation in air; h) electrical contact of the catalyst metal interconnected pattern to the electroplating electrode; i) seeded Au growth by electroplating.

The method is a promising low cost technology for producing high aspect ratio microstructures by surpassing the limits of other etching techniques, such as the crystal orientation of KOH wet etching<sup>[8]</sup> and the scalloped side walls of reactive ion etching.<sup>[9]</sup> Several research fields, such as microfluidics and bioengineering,<sup>[10]</sup> thermoelectric materials,<sup>[11]</sup> battery anodes,<sup>[12]</sup> black silicon<sup>[13]</sup> and solar cells,<sup>[13]</sup> sensors and MEMS technology,<sup>[14]</sup> photonic devices<sup>[15]</sup> and X-ray optics<sup>[16]</sup> can take advantage of using Pt-MacEtch as micro-fabrication technique. We address here the microfabrication of high aspect ratio structures for grating X-ray interferometry (GI).

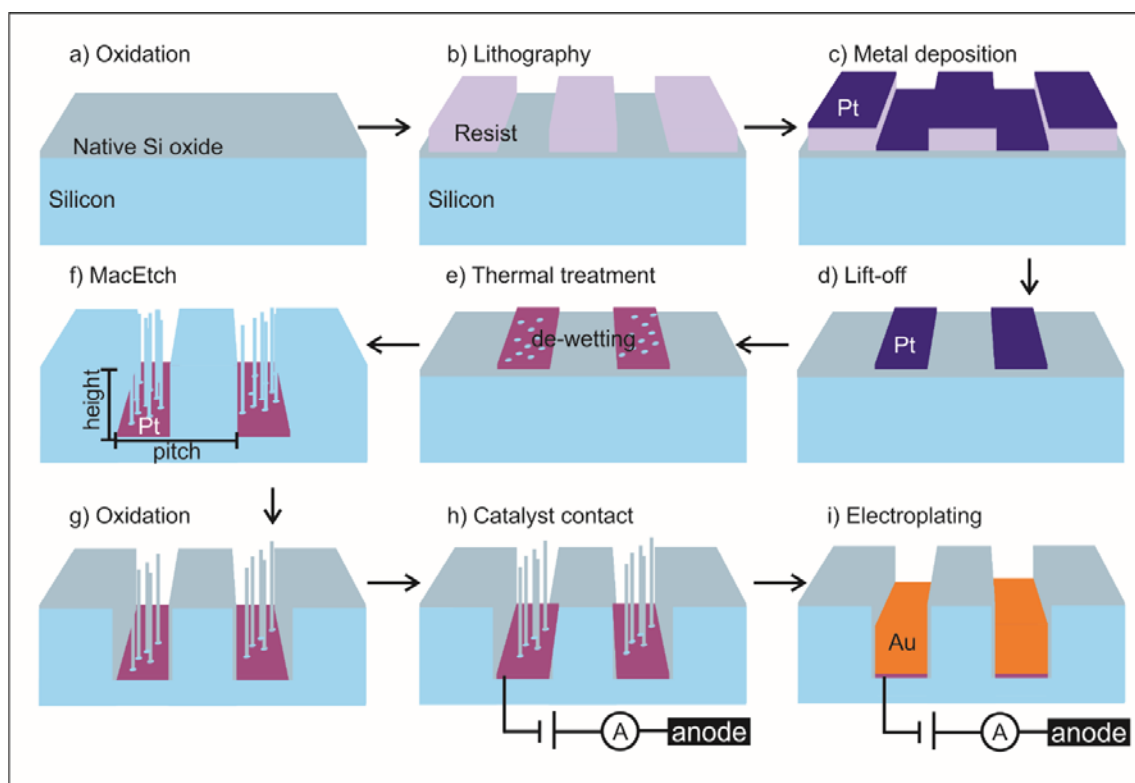


**Figure 1.** Schematic illustration of the grating fabrication process by MacEtch and subsequent Au electroplating. The Pt pattern works as a catalyst for MacEtch and a seed layer for Au electroplating.

## 2. Platinum thermal de-wetting

Submitted version (High aspect ratio grating microfabrication by Pt assisted chemical etching and Au electroplating, by L. Romano, J. Vila-Comamala, K. Jefimovs and M. Stampanoni, *Advanced Engineering Materials*, Copyright © 2020, Advanced Engineering Materials, Wiley-VCH Verlag GmbH & Co. KGaA) <https://doi.org/10.1002/adem.202000258>

The use of an interconnected nanoporous pattern has been demonstrated to be effective in reducing the off-vertical catalyst movement.<sup>[16-18]</sup> The nanopore morphology allows the MacEtch reactants to pass through the catalyst spacing, significantly improving the mass transport and uniformity, which ensures a highly uniform etch rate over the catalyst area. De-wetting occurs when a thin metal film on a solid substrate is heated, inducing breaking and reassembling of the film.<sup>[19, 20]</sup> The film morphology can be tuned as a function of film thickness and annealing temperature. The Pt de-wetting on native silicon oxide was investigated for film thickness in the range of 8-20 nm in the temperature range between 250 and 600 °C<sup>[19]</sup> by annealing in air to determine the best conditions for a robust interconnected pattern of the MacEtch catalyst. Native silicon oxide provides an oxygen terminated surface<sup>[21]</sup> that facilitates the metal film de-wetting and allows the formation of platinum silicide at the interface.<sup>[22]</sup> Platinum silicide improves the metal adhesion on the substrate, which prevents the catalyst peel-off when the sample is immersed in heavily concentrated HF solution.<sup>[7]</sup>

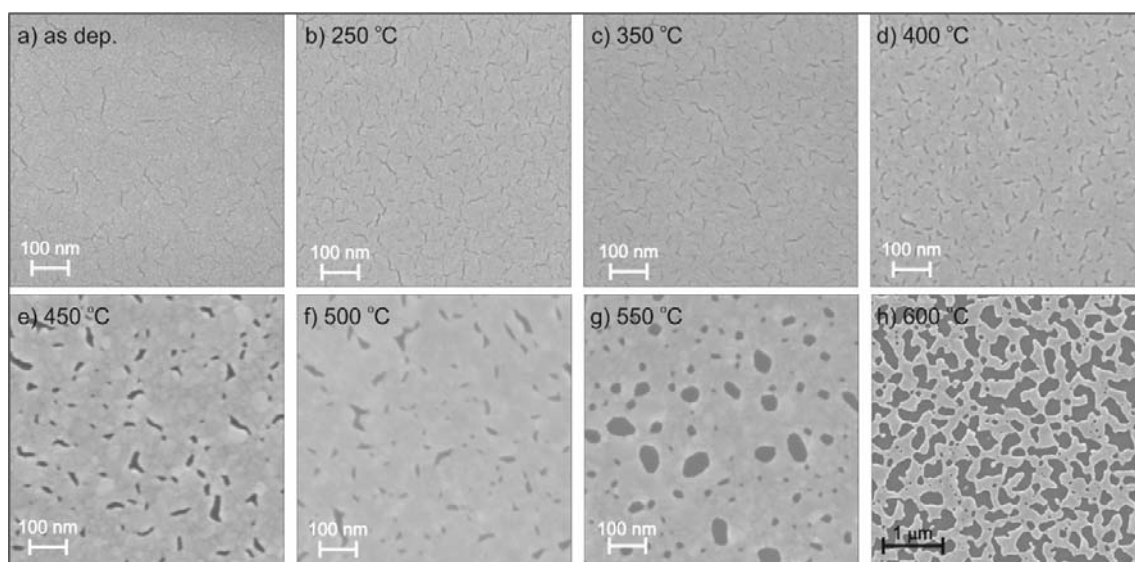


**Figure 2.** SEM in plan view of Pt film (12 nm) deposited on oxygen terminated Si surface (a) and annealed in air for 30 min at different temperatures (b-h) to form a metal de-wetted pattern.

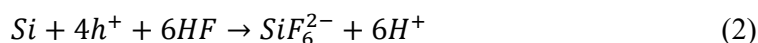
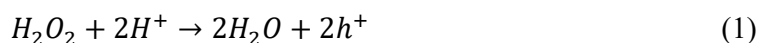
**Figure 2** reports a series of images by scanning electron microscopy (SEM) of a Pt film (12 nm) deposited on a Si substrate with a cleaned native oxide (only oxygen plasma was used to clean the surface before the deposition) and treated at different temperatures. The Pt de-wetting occurs in agreement with literature<sup>[20]</sup> with a progressive increase of film fractures (250 – 350 °C) leading to the hole formation (400 – 500 °C), and finally followed by holes coalescence and growth (550 – 600 °C). The film morphology has to be carefully chosen as a function of the upcoming etching.<sup>[18]</sup> The pattern at 250-350 °C shows still the presence of the initial cluster morphology so the film is less robust and cannot afford vertical etching.<sup>[17]</sup> The pattern at 400-450 °C has a compact morphology and a uniform distribution of holes so it gives the best pattern option for MacEtch. The growth of asymmetric holes during de-wetting is also an indication of Pt silicide formation.<sup>[20]</sup> In the high temperature range (500 – 600 °C) the presence of large asymmetric holes can create etching rate differences due to variation of the reactants diffusion, moreover MacEtch will produce nanowires with section size up to 100

nm that are difficult to remove at the end. The pattern at 600 °C shows disconnected particles that can potentially become a source of distortions during the etching<sup>[16]</sup> due to uncontrolled catalyst rotation.<sup>[6]</sup>

### 3. Metal assisted chemical etching

#### 3.1 Pt-MacEtch

Etching occurs when the Si substrate is immersed in a solution with an etchant (HF) and an oxidizer (H<sub>2</sub>O<sub>2</sub>), according to the following reactions:



where the reaction (1) occurs at the metal surface.

After metal de-wetting the Si substrates were cut in pieces of 1x1 cm<sup>2</sup> and etched in a liquid solution of HF and H<sub>2</sub>O<sub>2</sub>. The etching mechanism and the composition dependence have been extensively reported in literature.<sup>[2, 23, 24]</sup> MacEtch solutions are usually described in terms of concentrations ratio between HF and H<sub>2</sub>O<sub>2</sub>, according to Chartier's formula<sup>[23]</sup>

$$\rho = \frac{[HF]}{[HF]+[H_2O_2]} \quad (3)$$

where [HF] and [H<sub>2</sub>O<sub>2</sub>] are the molar concentration of HF and H<sub>2</sub>O<sub>2</sub>, respectively and

Hildreth's<sup>[25]</sup> compact expression  $\rho^x$ , where  $x=[HF]$ .

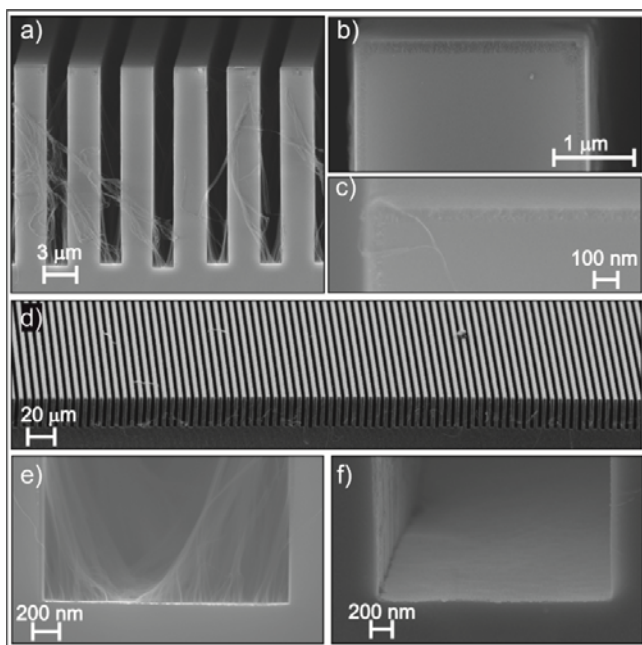


**Figure 3.** SEM in cross section of Pt assisted chemical etching of silicon grating with 4.8  $\mu\text{m}$  pitch (a, d), magnified view of the top (b) with etching solution  $\rho^{[\text{HF}]}=0.99^{20}$ . The etching time is 100 min. Magnified view of the top (c) with additional methanol (1.25 mol/L) in the etching solution. Magnified view of the bottom trench (e) just after the MacEtch and after removing nanowires (f).

**Figure 3** reports an example of MacEtch with nanoporous Pt layer as catalyst (Pt-MacEtch).

The images are scanning electron microscopy (SEM) in cross-section of a typical grating with pitch 4.8  $\mu\text{m}$ , duty cycle 0.5 and depth 18  $\mu\text{m}$ . The etching was performed by immersing the sample in an etching solution ( $\rho^{[\text{HF}]}=0.99^{20}$ ) for 100 min (etching rate 0.18  $\mu\text{m}/\text{min}$ ). The etching is vertical and uniform as showed in Figure 3 a-d. A magnified view of the top (Fig. 3 b) Si lamella shows very smooth side walls with tiny layer of microporous Si (100 nm thickness). The thickness of the microporous Si can be additionally reduced by adding a small amount of alcohol to the etching solution.<sup>[26]</sup> Fig. 3 c reports a magnified SEM of the top Si lamellas etched with the same solution of Fig. 3 b with additional methanol (1.25 mol/L, etching time 100 min), the microporous thickness is below 50 nm. We observed that methanol



is less affecting the etching rate with respect of isopropanol and ethanol alcohol, in agreement with literature results.<sup>[27]</sup> The bottom trench (Fig. 3 e) shows a flat profile of the Pt catalyst indicating that the etching occurred along the  $\langle 100 \rangle$  axis in a perpendicular direction to the Si substrate and that the catalyst is stable without deformation of the catalyst layer. This is a relevant feature and a prerequisite for high aspect ratio X-ray optics fabrication. Any deformation of the catalyst may affect the side wall slope that implies a variation of the duty cycle with the height. This impacts the final application of the grating, since the X-ray grating interferometry is very sensitive to the grating period and duty cycle.

The nanowires due to the etching with a nanoporous catalyst layer<sup>[28]</sup> are clearly visible in the bottom trench (Fig. 3 d). The Pt catalyst layer was 12 nm thick and annealed at 400 °C, the porous morphology before the etching is reported in the SEM of Figure 2 d and is constituted of elongated holes with section size in the range of 1-10 nm. The presence of nanowires in the etched trenches indicates that etching has the capability to etch microstructures with aspect ratio of 8:1 and nanostructures with aspect ratio of at least 1800:1 with the same etching rate. For some applications the nanowires in the bottom trenches can be completely removed by letting them oxidize in regular air (humidity 50 %) for a few days after the MacEtch and by dipping the sample in water diluted HF (wt 10%) for 20 min that easily etches away the silicon oxide. An example of the result of such process is shown in Fig. 3 e. The slow process of oxidation in air followed by HF etching of SiO<sub>2</sub> is preferred with respect to fast processing such as etching in solution of HNO<sub>3</sub> and HF in order to preserve the trench profile.

The volume of the etching solution has to be large enough to provide an almost constant supply of reactants, otherwise the etching rate decreases and finally the etching stops. We observed that for an etching solution with  $\rho^{[HF]}=0.96^{10}$  the etching rate varied from 0.20 to 0.15  $\mu\text{m}/\text{min}$  by reducing the solution volume from 100 ml to 50 ml. For this reason the

solution volume was fixed to 200 ml for sample size of 1 cm<sup>2</sup> and grating duty cycle of 0.5, which means that the catalyst area is about 0.5 cm<sup>2</sup>.

The effect of etchant consumption is particularly relevant for the etching with very high HF concentration. The <100> direction is observed to be the preferred etching direction since the number of Si back-bonds that have to be broken is the lowest. A significant reduction of the etching rate may suppress the vertical etching and allows etching towards other major crystallographic directions or some vector combinations of them. Chern et al.<sup>[29]</sup> suggested that a higher relative concentration of HF can allow etching in directions other than <100>, as HF becomes more readily available to remove the oxidized Si. Therefore if the H<sub>2</sub>O<sub>2</sub> concentration decreases during etching, the onset of etching along a different direction can be observed. This has been experimentally demonstrated in **Figure 4**, which shows (Fig. 4 a) a sample etched with  $\rho^{[\text{HF}]}=0.99^{28}$  (H<sub>2</sub>O<sub>2</sub> concentration 0.126 mol/L), the etching rate is about 0.05  $\mu\text{m}/\text{min}$  and the etching occurred along the <100> direction since the Pt catalyst layer at the bottom of the trench is flat.

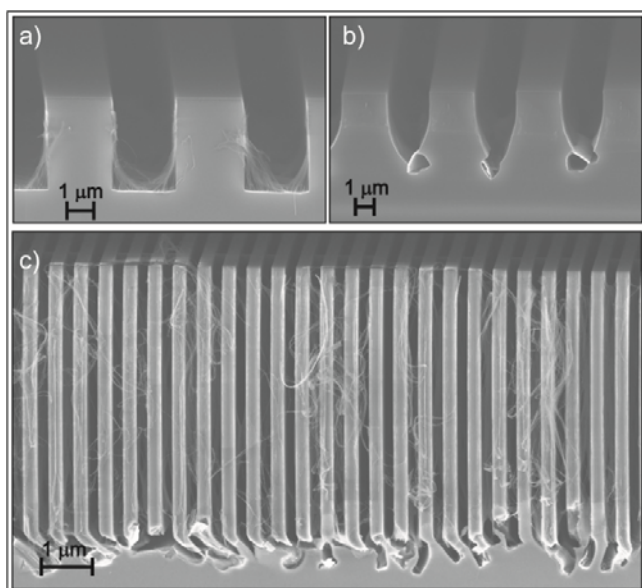


**Figure 4.** SEM in cross section of Pt assisted chemical etching of silicon grating with 4.8  $\mu\text{m}$  pitch, a) sample etched with  $\rho^{[\text{HF}]}=0.99^{28}$  (H<sub>2</sub>O<sub>2</sub> concentration 0.126 mol/L, etching time 60 Submitted version (High aspect ratio grating microfabrication by Pt assisted chemical etching and Au electroplating, by L. Romano, J. Vila-Comamala, K. Jefimovs and M. Stampanoni, Advanced Engineering Materials, Copyright © 2020, Advanced Engineering Materials, Wiley-VCH Verlag GmbH & Co. KGaA) <https://doi.org/10.1002/adem.202000258>

min); b) sample etched with  $\rho^{[\text{HF}]}=0.99^{10}$  ( $\text{H}_2\text{O}_2$  concentration 0.042 mol/L, etching time 180 min); c) sample that has been etched in a solution with  $\rho^{[\text{HF}]}=0.99^{20}$  and then washed for 10 min in a solution of deionized water and isopropanol alcohol in a ratio of 50:50.

Figure 4 b illustrates a sample etched with  $\rho^{[\text{HF}]}=0.99^{10}$  ( $\text{H}_2\text{O}_2$  concentration 0.042 mol/L), the etching rate slowed down to 0.02  $\mu\text{m}/\text{min}$  but the etching direction was  $\langle 100 \rangle$  only for the first 1.6  $\mu\text{m}$ , while the catalyst layer tilted and twisted evidencing a remarkable change of etching direction, presumably because the  $\text{H}_2\text{O}_2$  was fully consumed. The same phenomena can be observed when the etching slowing down is caused by the presence of a relevant amount of alcohol. Figure 4 c shows a sample that has been etched in a solution with  $\rho^{[\text{HF}]}=0.99^{20}$  and then washed for 10 min in a solution of deionized water and isopropanol alcohol in a ratio of 50:50. The washing process progressively diluted the etching solution inside the trenches. The presence of a relevant concentration of isopropanol alcohol slowed down the etching rate, thus favoring the tilt and the off-vertical etching in agreement with results reported by Kim et al. for nanowires.<sup>[27]</sup>

### 3.2 Au- versus Pt-MacEtch

Patterning microstructures requires high precision of pattern transfer and high lateral resolution during etching, with MacEtch this corresponds to a condition of very high HF concentration.<sup>[16]</sup> Au catalyst suffers of bad adhesion on silicon substrates and a detrimental pattern peel-off has been reported during MacEtch in conditions of high HF concentration.<sup>[30]</sup> On the contrary, uniform high aspect ratio have been reported for nonporous Au catalyst formed on native silicon oxide surface only in condition of low HF and high  $\text{H}_2\text{O}_2$  concentration,<sup>[17]</sup> where the effect of lateral etching causes a strong tapering<sup>[31]</sup> degrading the quality of the grating and making the process not usable for very high aspect ratio structures.

Platinum has the faster reported etching rate for MacEtch<sup>[5]</sup> due to its superior catalytic activity and has the advantage to form a stable silicide (PtSi and Pt<sub>2</sub>Si) on Si substrate at relatively low temperature (180-400 °C),<sup>[32]</sup> which ensures a robust adhesion of the metal with the Si substrate during MacEtch in conditions of high HF concentration.<sup>[7]</sup>

For deep trenches (> 20 μm) a high etching rate is desirable since the Si side walls are subjected to secondary undesired etching that degrades the trench profile. We wanted to discriminate which catalyst works better for the fabrication of high aspect ratio X-ray gratings. Au and Pt patterns with pitch size of 4.8 μm and duty cycle of 0.5 have been prepared for MacEtch according to the process of Figure 1. The etching conditions were selected in order to compare the best performances of each catalyst for etching the same type of grating (pitch 4.8 μm and height about 80 μm). The comparison of the processing is then functional to the grating quality. The etching parameters are reported in **table 1** for both catalysts.

**Table 1.** Grating with pitch 4.8 μm. MacEtch catalyst and etching parameters for Au and Pt of Figure 5.

Catalyst	Catalyst thickness [nm]	Annealing T [°C]	$\rho^{[HF]}$ <sup>a)</sup>	[H <sub>2</sub> O <sub>2</sub> ] [mol/L]	Isopropanol [mol/L]	Etching time [min]	Etching rate [μm/min]
Au	10	180	0.60 <sup>3,5</sup>	2.33	1.80	400	0.2
Pt	12	450	0.96 <sup>20</sup>	0.83	0.16	40	2.0

<sup>a)</sup>See reference Chartier et al.<sup>[23]</sup>;

The Au patterned sample was prepared and etched up to 80 μm, accordingly to previous report.<sup>[17]</sup> **Figure 5** reports some SEM images in cross-section of the gratings.

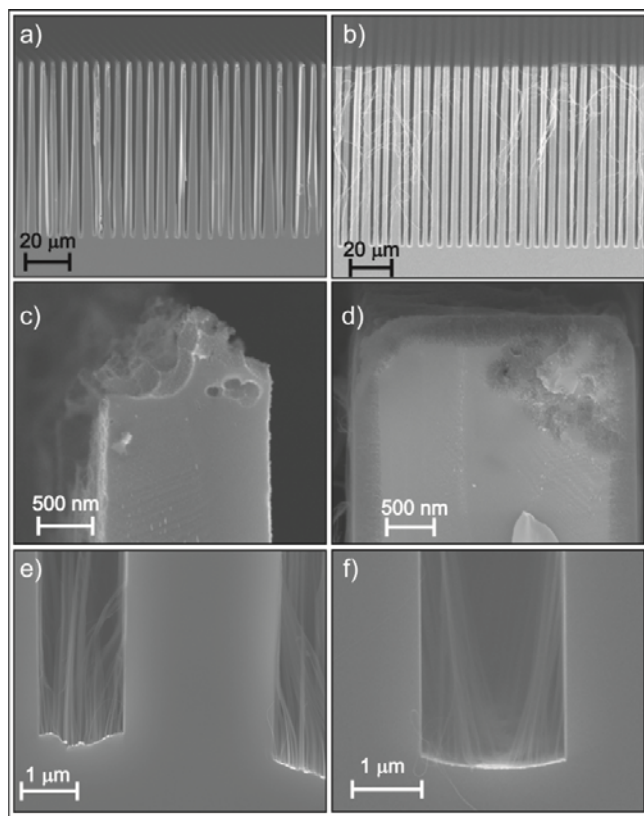


**Figure 5.** SEM in cross section of silicon gratings with 4.8  $\mu\text{m}$  pitch realized by MacEtch with Au (a, c, e) and Pt (b, d, f) as catalyst ( $\rho^{[\text{HF}]}=0.60^{3.5}$  and  $0.96^{20}$  for Au and Pt, respectively). The experiment conditions are reported in **Table 1**. Magnified view of the top (c, d) and the bottom (e, f).

The advantage of Pt-MacEtch is not only the etching rate – about 1 order of magnitude higher than Au-MacEtch – but also the reduced degradation of the trench profile. This is due to off-metal silicon etching. Once the oxidant is reduced on the surface of noble metal, holes are injected into the Si substrate. The holes diffuse from the Si under the noble metal to off-metal areas that may be etched and form microporous Si. The top and the bottom of the trenches are compared in Figure 5 c-d and e-f, respectively. The Si lamellas appear much thinner and damaged on top for Au with respect of Pt (Fig. 5 c-d). In the case of Au (Fig. 5 c) the top is much rougher due to the off-metal Si etching.

The off-metal etching is one of the main drawback of MacEtch, silicon is also etched faraway from the catalyst pattern.<sup>[33]</sup> Chartier et al.<sup>[23]</sup> described the formation of microporous Si on the side walls of the etched track of the metal particle as a consequence of the holes diffusion. In the model by Kolansinki et al.<sup>[34]</sup>, near the metal nanoparticle where the polarization is highest, etching is pushed into the electropolishing regime. Far from the nanoparticle, as the polarization drops off, microporous Si is formed.

The off-metal etching is relevant for the grating fabrication since it can deteriorate the Si trench profile. The top Si presents some macro-pores structure in the case of Au etch (Fig.5 c) and a more compact microporous layer in the case of Pt (Fig.5 d). Au-based experiments are actually 10 times longer than Pt ones and the microporous layer could have been etched away during the immersion in HF-H<sub>2</sub>O<sub>2</sub> solution. Chartier et al.<sup>[23]</sup> reported that Ag particles forms cone-shaped microporous Si pores and at the end of the treatment, the pores are empty because microporous Si is chemically etched by HF-H<sub>2</sub>O<sub>2</sub>. Since the etching solution of Au contains a lower concentration of HF and the H<sub>2</sub>O<sub>2</sub> concentration is 3 times higher with respect of Pt case, the rate of hole consumption at the Si/metal interface is smaller than the rate of holes injection, causing a higher concentration of diffusing holes to off-metal areas. The formation of macro-pits could be a consequence of the different holes injection rate and the speed of catalyst movement inside the Si wafer. In the case of Pt, there are less macro-pits and the microporous layer looks more resistant to further etching, resulting in a better trench profile, even after long etching time, as showed by the results in the section 3.3. As a conclusion, a faster etching with the smallest amount of H<sub>2</sub>O<sub>2</sub> is preferable to reduce the off-metal etching that degrades the grating quality. The bottom profile of the trenches is much more tilted in the case of Au with respect of Pt. This means that the Au pattern is subjected to bend and stretch during the etching, with consequent distortion of the pattern. Both Au and Pt

bottom profiles show tiny nanowires which are consequence of the metal de-wetting that creates a porous catalyst layer. The nanowires tend to collapse by capillary force on the neighbour Si side walls during the liquid drying. This issue is a well-known drawback of wet-etching techniques and it can be solved by applying freezing drying or critical point drying steps after the etching. It is also relevant for microstructures once the aspect ratio is higher than 20:1.

### 3.3 High aspect ratio gratings

With the increase of grating height, the Si lamellas can bend and collapse on the top part of the grating during the liquid drying at the end of the etching process. **Figure 6** reports some examples of deep trenches realized by Pt-MacEtch, Figure 6 a shows a grating with pitch 4.8  $\mu\text{m}$  and height greater than 100  $\mu\text{m}$ , the top of the Si lamellas stick together distorting the grating periodicity. In order to prevent such issue, the pattern was modified by adding some transversal connecting structures (bridges) that hold the thin Si lamellas during the drying step. This minimizes the risk of pattern distortion during the drying step. Figure 6 b-c reports the SEM cross-section of gratings with bridges with pitch 4.8 and 10  $\mu\text{m}$ , respectively. The relative catalyst patterns are showed in Figure 6 d-e (Pt pattern is in bright contrast after lift-off). Both designs (Figure 6 d-e) prevent the lamellas to collapse and distort during drying. The pattern of Figure 6 e has less impact in the GI application of the grating. Moreover, the pattern was designed in a way to ensure the catalyst interconnection and to minimize eventual distortions of the metal film during the etching.<sup>[16]</sup>

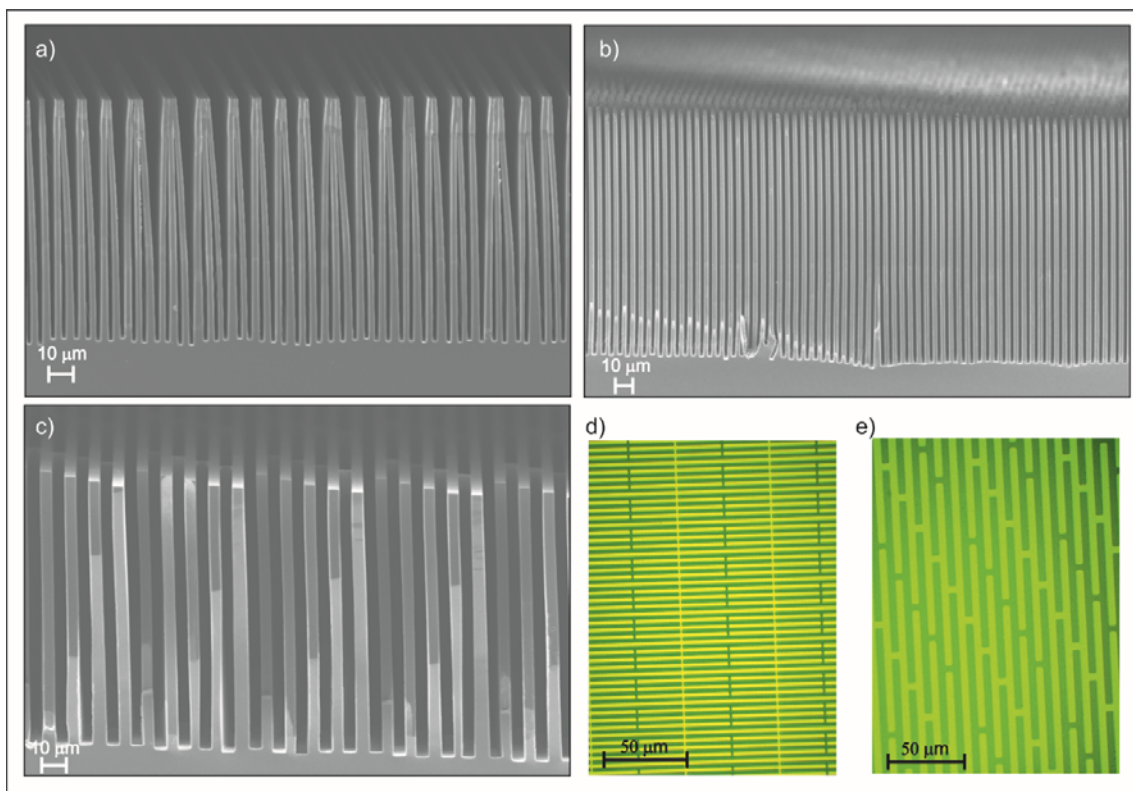


**Figure 6.** SEM in cross section of high aspect ratio silicon gratings without (a) and with silicon bridges (b, c), the catalyst geometries are showed in (d-e), respectively. Different Pt patterns were designed to implement the catalyst interconnection and the silicon bridges, optical images in plan view of Pt pattern (Pt is bright, Si is dark) after lift-off (d, e). Etching conditions: a)  $\rho^{[\text{HF}]}=0.96^{5,3}$ ,  $[\text{H}_2\text{O}_2]=0.22$  mol/L, 400 min; b)  $\rho^{[\text{HF}]}=0.99^{20}$ ,  $[\text{H}_2\text{O}_2]=0.20$  mol/L, 800 min c)  $\rho^{[\text{HF}]}=0.98^{17}$ ,  $[\text{H}_2\text{O}_2]=0.38$  mol/L, 155 min.

The grating of Figure 6 b (pitch  $4.8 \mu\text{m}$ , height  $145 \mu\text{m}$ ) has aspect ratio of 60:1, it was etched with  $\rho^{[\text{HF}]}=0.99^{20}$  and etching rate of about  $0.18 \mu\text{m}/\text{min}$ . The grating of Figure 6 c (pitch  $10 \mu\text{m}$ , height  $110 \mu\text{m}$ ) has an aspect ratio of 22:1; it was etched with  $\rho^{[\text{HF}]}=0.98^{17}$  and etching rate of about  $0.7 \mu\text{m}/\text{min}$ .

The Pt-MacEtch of deep trenches has been optimized as a function of etching rate for high aspect ratio structures and quality of the pattern transfer from the initial photolithographic mask to the Si substrate. In comparison to the other wet etching techniques,<sup>[8]</sup> Pt-MacEtch



demonstrated the capability to etch very high aspect ratio with a good control of the trench profile and height.

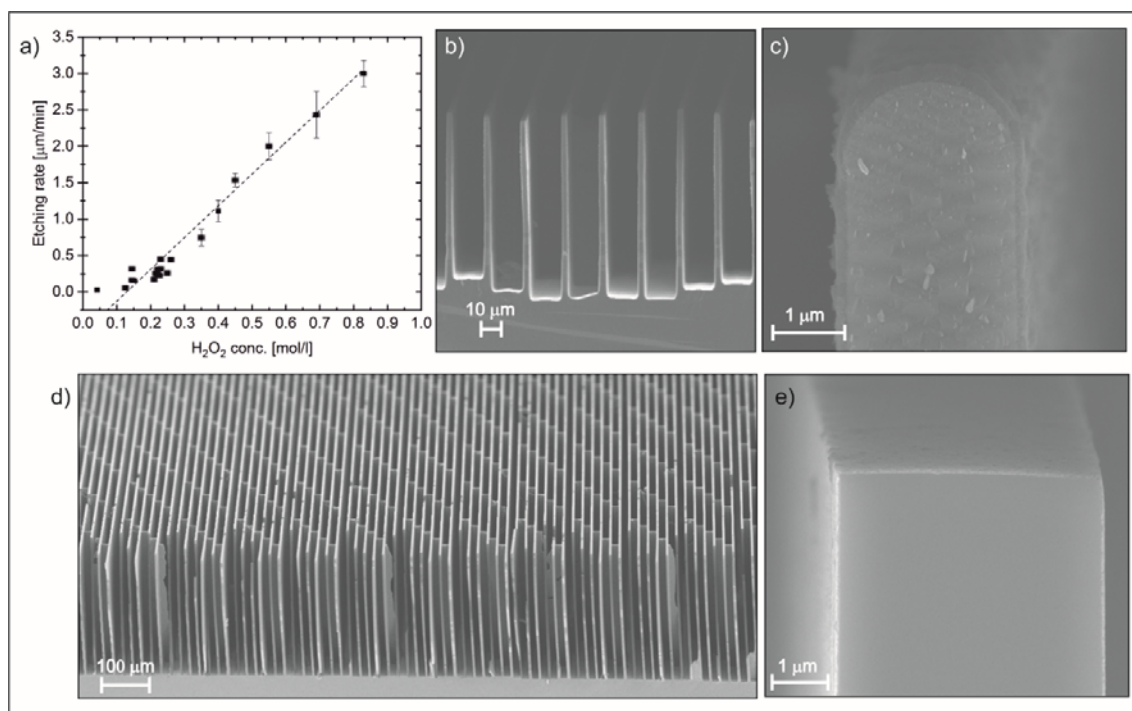


**Figure 7.** Etching rate versus  $\text{H}_2\text{O}_2$  concentration (a) for gratings with pitch  $20\ \mu\text{m}$  and duty cycle  $0.25$  (Pt line width  $15\ \mu\text{m}$ , Si gap width  $5\ \mu\text{m}$ ). SEM cross section of grating etched with  $\rho^{[\text{HF}]}=0.85^5$  and  $\text{H}_2\text{O}_2$  concentration of  $0.83\ \text{mol/L}$  for  $30\ \text{min}$  (b, c) and  $\rho^{[\text{HF}]}=0.96^6$  and  $\text{H}_2\text{O}_2$  concentration of  $0.25\ \text{mol/L}$  for  $960\ \text{min}$  (d, e). All the solutions contain methanol at  $1.25\ \text{mol/L}$ .

**Figure 7** reports the results of a study conducted on grating structures with pitch  $20\ \mu\text{m}$  and duty cycle  $0.25$  (Pt line width  $15\ \mu\text{m}$ , Si gap width  $5\ \mu\text{m}$ ). Since the etching occurs in a concentration regime ( $\rho > 0.85$ ) where the limiting factor is the oxidant concentration, the etching rate is reported as a function of  $\text{H}_2\text{O}_2$  concentration (Fig. 7 a). For  $\text{H}_2\text{O}_2$  concentration higher than  $0.8\ \text{mol/L}$  the etching rate is about  $3\ \mu\text{m/min}$  but the etching depth is not uniform (Fig. 7 b) and the top Si lamella profile (Fig. 7 c) is quite tapered ( $2.7\ \mu\text{m}$ ) for a grating height of  $90\ \mu\text{m}$ . With  $\text{H}_2\text{O}_2$  concentration of  $0.25\ \text{mol/L}$  the etching rate drops to  $0.26\ \mu\text{m/min}$  (Fig.

7 d) but the top Si lamella profile (Fig. 7 e) has still width of 4.7  $\mu\text{m}$  for a grating height of 250  $\mu\text{m}$ . Therefore this last example represents a good compromise for etching very deep structures with a good quality of the trench profile. An amount of 3.5 l of this etching solution ( $\rho^{[\text{HF}]}=0.96^6$ ) was used to produce a grating of 8x4  $\text{cm}^2$  on a 4 inches wafer. The solution was slowly stirred (50 rpm) as suggested by Li et al. [35] during the etching time of 16 h. The scatter of the data for the low  $\text{H}_2\text{O}_2$  concentration (Fig. 7 a) is due to a slight dependence on the HF concentration and to the fact that etching very deep structures requires the diffusion of fresh reactants into the deep trenches as long as the etching proceeds. The etching rate progressively slows down due to the limited diffusion of reactants, so the etching time has to be carefully tuned as a function of the desired height.

#### 4. Seed gold electroplating

For the hard X-ray regime, the Pt-MacEtch gratings can be combined with metallization techniques. The presence of metal catalyst layer at the bottom of the etched structures offers the possibility to use the same as a metallization contact for the subsequent Au electroplating step. With respect to other approaches of damascene process, [36] the seed growth from the bottom [37, 38] does not need any additional step of conformal metallization [39] and allows to create a compact Au filling [40] independently of aspect ratio. [41]

The Pt catalyst was designed to have a full interconnected pattern that can be used as a metallization for seed growing of Au by electroplating (Fig. 1 h). The Si trenches were oxidized in air so that they became electrically isolated [38] and thus promoting the growth of Au from the bottom of the trench. Since the Pt-MacEtch grating has a thick conformal porous layer, the growth of native Si oxide (Fig. 1 g) is enough to avoid the Au growth on the side walls during the electroplating. **Figure 8** shows the progressive filling of the grating trenches

Submitted version (High aspect ratio grating microfabrication by Pt assisted chemical etching and Au electroplating, by L. Romano, J. Vila-Comamala, K. Jefimovs and M. Stampanoni, Advanced Engineering Materials, Copyright © 2020, Advanced Engineering Materials, Wiley-VCH Verlag GmbH & Co. KGaA) <https://doi.org/10.1002/adem.202000258>

starting from the bottom (Fig. 8 a). The seed layer was the Pt catalyst as demonstrated in Figure 8 b, where the Pt catalyst pattern with de-wetting features (see Fig. 2) is clearly recognizable at the bottom of the Au electroplated film. The residual nanowires are incorporated into the Au layer (Fig. 8 a) and they do not affect the trench full filling (Fig. 8 c). Since the nanowires are very thin, their volume fraction is negligible for the application of the Au electroplated structures as X-ray absorption grating in GI.

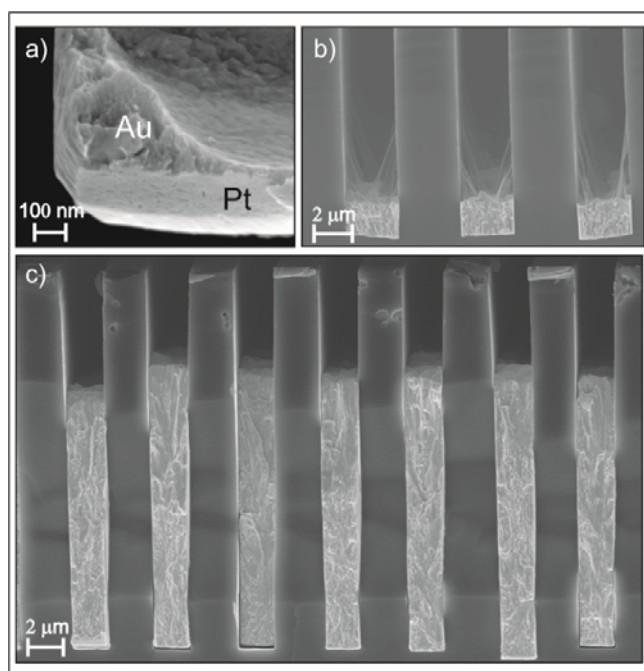


**Figure 8.** SEM cross section of gratings after Au electroplating. The electroplating has been interrupted at different stages to monitor the Au growth. In a first stage Pt catalyst is recognizable as seed layer with the typical de-wetting pattern of Pt (a). In a second stage the Au growth is observed at the bottom of the trenches (b). In a third stage (c) Au continues to grow with a progressive filling of the trenches (c).

## 5. X-ray gratings phase interferometry

X-ray grating interferometry<sup>[42]</sup> can access to phase and scattering contrasts with conventional X-ray sources,<sup>[43]</sup> thus facilitating the potential for medical<sup>[44]</sup> and industrial applications.<sup>[45]</sup>

Gratings with micrometre sized periods that modulate the phase or the intensity of the X-rays

are challenging and expensive to fabricate.<sup>[46]</sup> Efficiency of X-ray diffractive elements is strictly dependent on precision of the pitch and uniformity of duty cycle along the depth. This is possible only if the side wall slope of the etched structures is perpendicular to the Si wafer substrate and the Au filling is compact and homogenous. Gratings microfabrication by means of Pt-MacEtch and subsequent Au electroplating represents a robust and cost-efficient fabrication route. Using MacEtch, we successfully fabricated gratings that are used in a laboratory-GI setup. The use of the gratings in GI experiments will be reported separately. Here, the focus is on the viability of the fabrication and the possible impact of inhomogeneous Au filling that cannot be detected in SEM characterization.

Due to the X-ray source characteristics, X-ray grating interferometry systems typically consist of a combination of two<sup>[47]</sup> (synchrotron-based setups) or three X-ray gratings<sup>[48]</sup> (laboratory-based systems). In the latter case, the system consists of a source absorbing grating (G0), a phase grating (G1), and an analyzer absorbing grating (G2). In particular, the performance of Au filled grating with pitch of 6  $\mu\text{m}$  was investigated in a X-ray interferometer<sup>[48]</sup> for a design photon energy of 20 keV at the 3<sup>rd</sup> Talbot order and  $\pi/2$  phase shifting G1 grating. The Pt-MacEtch grating (pitch 6  $\mu\text{m}$ , height 39  $\mu\text{m}$ ) filled with Au up to 30  $\mu\text{m}$  was used as G0 grating. The G1 phase grating was made of Si by deep reactive ion etching (DRIE) and the G2 absorbing grating was fabricated by DRIE and Au electroplating. The manufacturing details of G1 and G2 gratings are reported elsewhere.<sup>[38]</sup> The interference fringe visibility is a common figure of merit in designs of X-ray grating-based interferometers.<sup>[49]</sup> The visibility depends on grating's phase shift, X-ray spectrum, spatial coherence degree of X-ray illumination, and system geometry, such as the phase grating to detector distance.<sup>[49]</sup> We measured an average X-ray fringe visibility of 17.5 % with  $\pi/2$  phase shift, which is

comparable to the values achieved in absorbing gratings fabricated by conventional DRIE followed by Au electroplating. [38]

The visibility map (visibility at each X-ray camera pixel) and differential phase contrast and scattering images of sample consisting of a grain ear are shown in **Figure 9**. The good quality of such fabricated grating is noticeable in the obtained almost defect free images of the sample.

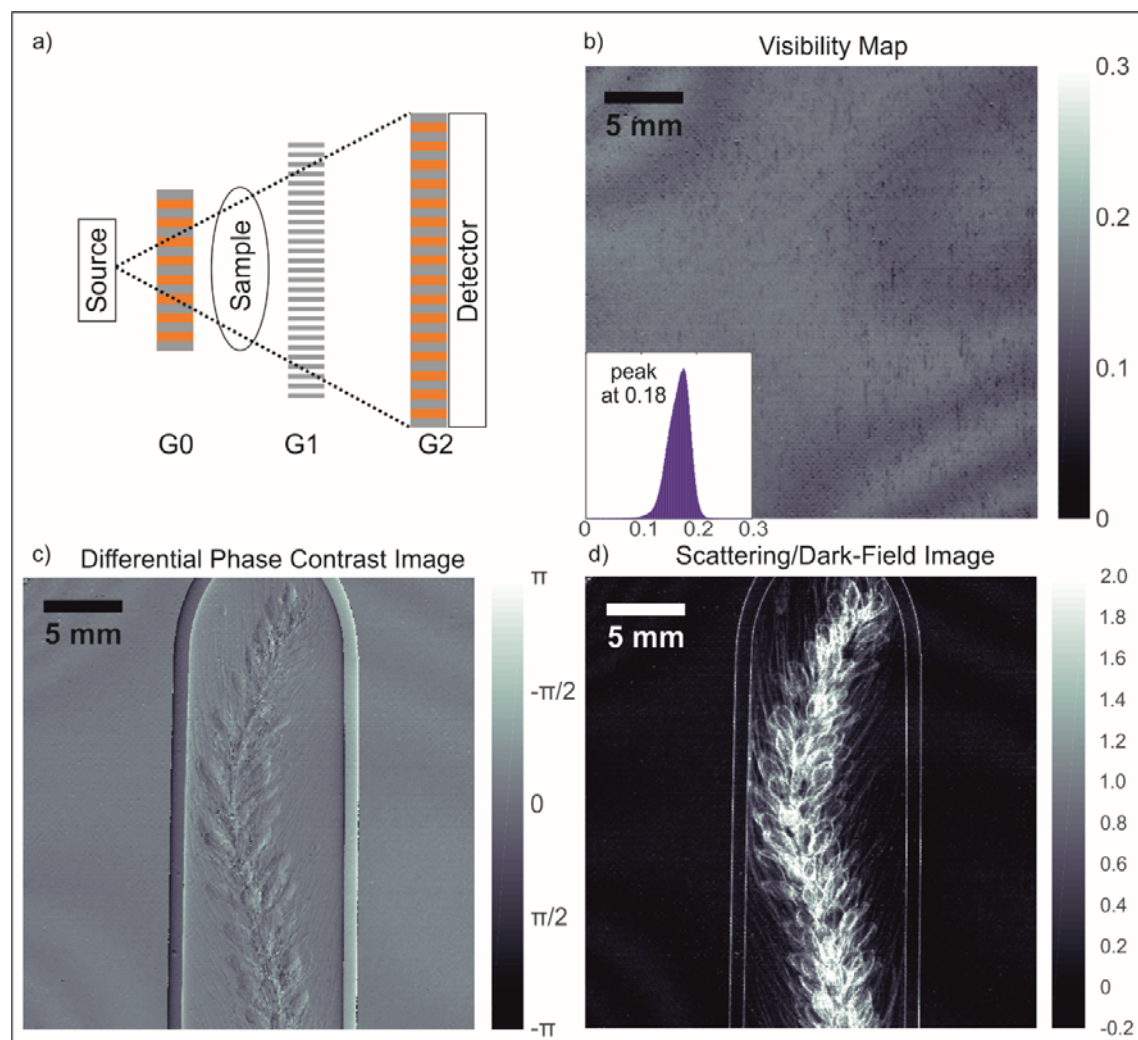


**Figure 9.** X-ray performance of a Au electroplated grating of 6  $\mu\text{m}$  period used as a G0 absorbing grating. Schematic (not to scale) of the X-ray interferometer (a); X-ray fringe visibility map with the visibility histogram in insert (b); differential phase contrast (c) and scattering (d) images of a grain ear.

Submitted version (High aspect ratio grating microfabrication by Pt assisted chemical etching and Au electroplating, by L. Romano, J. Vila-Comamala, K. Jefimovs and M. Stampanoni, Advanced Engineering Materials, Copyright © 2020, Advanced Engineering Materials, Wiley-VCH Verlag GmbH & Co. KGaA) <https://doi.org/10.1002/adem.202000258>

## 6. Conclusion

We demonstrated a full process of gratings microfabrication for X-ray interferometry by using Pt as catalyst for MacEtch in solution of HF and H<sub>2</sub>O<sub>2</sub> and subsequent Au electroplating. The application of metal de-wetting technique was used to create a porous catalyst layer that allows to etch very high aspect ratio structures with the advantage of the formation of platinum silicide that stabilize the catalyst and allows to access MacEtch with very high HF content in wet etching. The pattern design and the etching conditions have been studied in details as a function of the metal thermal treatment, the etching rate and the quality of the structures to optimize the process for different patterning requirements. We discussed the critical role of etching solution volume by showing the effect of reactants depletion and of the presence of alcohol additives, such as methanol and isopropanol. A small amount of alcohol can help to reduce the formation of the microporosity on the side wall trenches but does not substantially affect the etching rate. The H<sub>2</sub>O<sub>2</sub> depletion and the addition of alcohol can drastically change the etching direction due to the slowing down of the etching rate. The Pt catalyst layer that sinks down into the Si substrate during MacEtch has been successfully used as seed layer for Au electroplating in order to fabricate a periodic structure with an high absorbing material for hard X-ray. In this study, the metal catalyst used for MacEtch of Si is reused as a metallization contact for the Au electroplating. This definitely facilitates the fabrication step of absorbing gratings for GI, avoiding additional atomic layer deposition processes or complex electroplating approaches. The performance of the Au electroplated grating in terms of uniformity and quality of the filling have been assessed by using an X-ray interferometric set up at 20 keV.

## 7. Experimental Section

All samples were prepared from <100> n-type Si 4 inch wafers (resistivity 1-30  $\Omega\text{cm}$ ). All the wafers come from the same batch with this resistivity range. The wafers were processed according to the following sequence: 1) long oxygen plasma cleaning; 2) resist spin coating and lithographic process; 3) resist development; 4) short oxygen plasma cleaning; 5) Pt deposition; 6) lift-off; 7) thermal treatment; 9) MacEtch.

The long oxygen plasma cleaning (typically 5 minutes with oxygen RF plasma ashing) before the Pt deposition was to ensure the oxygen terminated Si surface for the metal thermal de-wetting. The short plasma cleaning (typically 10-60 s with oxygen RF plasma ashing) was used to clean the resist residuals, with the time being tuned to avoid an excessive thinning of the resist. Positive photoresist MICROPOSIT™ S1805 was spin-coated for photolithography, according to a procedure reported elsewhere.<sup>[17]</sup> Pt was deposited using an electron beam evaporator with a deposition rate of 0.5 nm/min. We performed depositions with Pt thickness in the range of 8-20 nm.

Lift-off was performed by dipping the samples in solvent with eventual ultrasonic agitation. The samples were finally dried by nitrogen blowing.

The thermal treatment was performed on a hot plate in air with a top cover, the annealing time at the set point was 30 min. The thermal de-wetting of Pt was investigated in the temperature range of 250 – 600 °C.

The liquid solution was prepared by mixing different volumes of water diluted HF (49 wt%), water diluted H<sub>2</sub>O<sub>2</sub> (30 wt%) and deionized water (18 M $\Omega$  cm). The total liquid volume of etchant was fixed to 200 ml for grating size of 1x1 cm<sup>2</sup> and patterned area of 0.5 cm<sup>2</sup>. For larger patterned area the solution volume was scaled up in order to maintain the volume/patterned area ratio of 0.2 l/cm<sup>2</sup>. MacEtch experiments were performed in opaque

Submitted version (High aspect ratio grating microfabrication by Pt assisted chemical etching and Au electroplating, by L. Romano, J. Vila-Comamala, K. Jefimovs and M. Stampanoni, Advanced Engineering Materials, Copyright © 2020, Advanced Engineering Materials, Wiley-VCH Verlag GmbH & Co. KGaA) <https://doi.org/10.1002/adem.202000258>

Teflon beaker with top cover in order to prevent illumination during the etching. Alcohol additives (methanol, isopropanol or ethanol up to 1.8 mol/L) were added to eventually reduce the side wall microporosity. After etching, the samples were rinsed in water and dried by nitrogen blowing. We recommend to follow all the necessary safety protocols in order to handle heavily concentrated HF.

Plan view and cross-section images of the samples were taken using the In-Lens detector of a Zeiss Supra VP55 Scanning Electron Microscope (SEM).

For the electroplating step, the metal contact on the grating was realized by evaporating a Cr/Au layer (10 nm Cr and 50 nm Au) in a small area on the front of the wafer. Si lamellas were electrically isolated by oxidizing them in regular air (humidity 50 %) during a few days after the MacEtch. The current density was 5 mA/cm<sup>2</sup>. Au electroplating was performed few days after MacEtch in Gold Potassium Cyanide bath (AUTRONEX GVC) at 45 °C.

The X-ray performance of the Pt-MacEtch grating filled with Au with a pitch of 6 μm was investigated by setting up a laboratory X-ray grating interferometry system using a Hamamatsu L10101 X-ray microsource (40 kV voltage and 0.2 mA electron current) and Hamamatsu Flat Panel C7942CA-22 detector (a region of interest of 1100x1100 pixels of 48 μm was used). The total length of the system was 87.1 cm, the design photon energy was 20 keV at the 3<sup>rd</sup> Talbot order and  $\pi/2$  phase shift. The system was built by mounting a set of 3 gratings on a high precision stage as showed in the schematic of Figure 9 a. The G0 grating had a pitch 6 μm and the Au height 30 μm, the grating area is 2×2 cm<sup>2</sup>. G1 and G2 gratings were fabricated by a method described by M. Kagias et al. [38] and had grating area of 7x7 cm<sup>2</sup> and pitch 3 and 6 μm, respectively. The grating interferometer visibility was calculated following the well-established method of Fourier analysis reported by Momose et al. [42]

#### Acknowledgements

Submitted version (High aspect ratio grating microfabrication by Pt assisted chemical etching and Au electroplating, by L. Romano, J. Vila-Comamala, K. Jefimovs and M. Stampanoni, Advanced Engineering Materials, Copyright © 2020, Advanced Engineering Materials, Wiley-VCH Verlag GmbH & Co. KGaA) <https://doi.org/10.1002/adem.202000258>



We would like to thank D. Marty and M. Bednarzik (PSI-LMN) for technical support. We acknowledge the support from: SNF Sinergia Grant CRSII5\_18356 “Clinical GI-BCT”, EU Grant ERC-2012-StG 31’0005 “PhaseX”, ERC-2016-PoC 727246 “Magic”, Eurostar Grant E!1106 “INFORMAT”, SNI NanoArgovia Grant 13.01 “NANOCREATE” and the lottery fund SwissLOS of the Kanton of Aargau.

Received: ((will be filled in by the editorial staff))

Revised: ((will be filled in by the editorial staff))

Published online: ((will be filled in by the editorial staff))

## Figures

**Figure 1.** Schematic illustration of the grating fabrication process by MacEtch and subsequent Au electroplating. The Pt pattern works as a catalyst for MacEtch and a seed layer for Au electroplating.

**Figure 2.** SEM in plan view of Pt film (12 nm) deposited on oxygen terminated Si surface (a) and annealed in air for 30 min at different temperatures (b-h) to form a metal de-wetted pattern.

**Figure 3.** SEM in cross section of Pt assisted chemical etching of silicon grating with 4.8  $\mu\text{m}$  pitch (a, d), magnified view of the top (b) with etching solution  $\rho^{[\text{HF}]}=0.99^{20}$ . The etching time is 100 min. Magnified view of the top (c) with additional methanol (1.25 mol/L) in the etching solution. Magnified view of the bottom trench (e) just after the MacEtch and after removing nanowires (f).

**Figure 4.** SEM in cross section of Pt assisted chemical etching of silicon grating with 4.8  $\mu\text{m}$  pitch, a) sample etched with  $\rho^{[\text{HF}]}=0.99^{28}$  ( $\text{H}_2\text{O}_2$  concentration 0.126 mol/L, etching time 60 min); b) sample etched with  $\rho^{[\text{HF}]}=0.99^{10}$  ( $\text{H}_2\text{O}_2$  concentration 0.042 mol/L, etching time 180 min); c) sample that has been etched in a solution with  $\rho^{[\text{HF}]}=0.99^{20}$  and then washed for 10 min in a solution of deionized water and isopropanol alcohol in a ratio of 50:50.

**Figure 5.** SEM in cross section of silicon gratings with 4.8  $\mu\text{m}$  pitch realized by MacEtch with Au (a, c, e) and Pt (b, d, f) as catalyst ( $\rho^{[\text{HF}]}=0.60^{3.5}$  and  $0.96^{20}$  for Au and Pt, respectively). The experiment conditions are reported in **Table 1**. Magnified view of the top (c, d) and the bottom (e, f).

**Figure 6.** SEM in cross section of high aspect ratio silicon gratings without (a) and with silicon bridges (b, c), the catalyst geometries are showed in (d-e), respectively. Different Pt patterns were designed to implement the catalyst interconnection and the silicon bridges, optical images in plan view of Pt pattern (Pt is bright, Si is dark) after lift-off (d, e). Etching conditions: a)  $\rho^{[\text{HF}]}=0.96^{5.3}$ ,  $[\text{H}_2\text{O}_2]=0.22$  mol/L, 400 min; b)  $\rho^{[\text{HF}]}=0.99^{20}$ ,  $[\text{H}_2\text{O}_2]=0.20$  mol/L, 800 min c)  $\rho^{[\text{HF}]}=0.98^{17}$ ,  $[\text{H}_2\text{O}_2]=0.38$  mol/L, 155 min.

**Figure 7.** Etching rate versus  $\text{H}_2\text{O}_2$  concentration (a) for gratings with pitch 20  $\mu\text{m}$  and duty cycle 0.25 (Pt line width 15  $\mu\text{m}$ , Si gap width 5  $\mu\text{m}$ ). SEM cross section of grating etched with  $\rho^{[\text{HF}]}=0.85^5$  and  $\text{H}_2\text{O}_2$  concentration of 0.83 mol/L for 30 min (b, c) and  $\rho^{[\text{HF}]}=0.96^6$  and  $\text{H}_2\text{O}_2$  concentration of 0.25 mol/L for 960 min (d, e). All the solutions contain methanol at 1.25 mol/L.

**Figure 8.** SEM cross section of gratings after Au electroplating. The electroplating has been interrupted at different stages to monitor the Au growth. In a first stage Pt catalyst is recognizable as seed layer with the typical de-wetting pattern of Pt (a). In a second stage the Au growth is observed at the bottom of the trenches (b). In a third stage (c) Au continues to grow with a progressive filling of the trenches (c).

**Figure 9.** X-ray performance of a Au electroplated grating of 6  $\mu\text{m}$  period used as a G0 absorbing grating. Schematic (not to scale) of the X-ray interferometer (a); X-ray fringe visibility map with the visibility histogram in insert (b); differential phase contrast (c) and scattering (d) images of a grain ear.

**Table 1.** Grating with pitch 4.8  $\mu\text{m}$ . MacEtch catalyst and etching parameters for Au and Pt of Figure 5.

Catalyst	Catalyst thickness [nm]	Annealing T [°C]	$\rho^{(\text{HF})}$ a)	[H <sub>2</sub> O <sub>2</sub> ] [mol/L]	Isopropanol [mol/L]	Etching time [min]	Etching rate [ $\mu\text{m}/\text{min}$ ]
Au	10	180	0.60 <sup>3,5</sup>	2.33	1.80	400	0.2
Pt	12	450	0.96 <sup>20</sup>	0.83	0.16	40	2.0

a) See reference Chartier et al.<sup>[23]</sup>;

## References

- [1] X. Li, P. W. Bohn, *Applied Physics Letters* 2000, 77, 2572.
- [2] Z. Huang, N. Geyer, P. Werner, J. de Boor, U. Gösele, *Advanced Materials* 2011, 23, 285.
- [3] D. Zhan, L. Han, J. Zhang, Q. He, Z.-W. Tian, Z.-Q. Tian, *Chemical Society Reviews* 2017, 46, 1526; B. Ki, Y. Song, K. Choi, J. H. Yum, J. Oh, *ACS Nano* 2018, 12, 609; S. Bastide, E. Torralba, M. Halbwx, S. Le Gall, E. Mpogui, C. Cachet-Vivier, V. Magnin, J. Harari, D. Yarekha, J.-P. Vilcot, *Frontiers in Chemistry* 2019, 7.
- [4] K. Tsujino, M. Matsumura, *Electrochemical and Solid-State Letters* 2005, 8, C193; X. Li, Y. Xiao, C. Yan, K. Zhou, S. L. Schweizer, A. Sprafke, J.-H. Lee, R. B. Wehrspohn, *ECS Solid State Letters* 2013, 2, P22; C.-L. Lee, K. Tsujino, Y. Kanda, S. Ikeda, M. Matsumura, *Journal of Materials Chemistry* 2008, 18, 1015; S. Chattopadhyay, X. Li, P. W. Bohn, *Journal of Applied Physics* 2002, 91, 6134.
- [5] S. Yae, Y. Morii, N. Fukumuro, H. Matsuda, *Nanoscale Research Letters* 2012, 7, 352.
- [6] O. J. Hildreth, K. Rykaczewski, A. G. Fedorov, C. P. Wong, *Nanoscale* 2013, 5, 961.

Submitted version (High aspect ratio grating microfabrication by Pt assisted chemical etching and Au electroplating, by L. Romano, J. Vila-Comamala, K. Jefimovs and M. Stampanoni, *Advanced Engineering Materials*, Copyright © 2020, Advanced Engineering Materials, Wiley-VCH Verlag GmbH & Co. KGaA) <https://doi.org/10.1002/adem.202000258>

- [7] L. Romano, M. Kagias, J. Vila-Comamala, K. Jefimovs, L.-T. Tseng, V. A. Guzenko, M. Stampanoni, *Nanoscale Horizons* 2020.
- [8] P. S. Finnegan, A. E. Hollowell, C. L. Arrington, A. L. Dagel, *Materials Science in Semiconductor Processing* 2019, 92, 80.
- [9] K. Ishikawa, K. Karahashi, T. Ishijima, S. I. Cho, S. Elliott, D. Hausmann, D. Mocuta, A. Wilson, K. Kinoshita, *Japanese Journal of Applied Physics* 2018, 57, 06JA01.
- [10] C. Chiappini, P. Campagnolo, C. S. Almeida, N. Abbassi-Ghadi, L. W. Chow, G. B. Hanna, M. M. Stevens, *Advanced Materials* 2015, 27, 5147.
- [11] A. I. Boukai, Y. Bunimovich, J. Tahir-Kheli, J.-K. Yu, W. A. Goddard Iii, J. R. Heath, *Nature* 2008, 451, 168.
- [12] M. R. Zamfir, H. T. Nguyen, E. Moyon, Y. H. Lee, D. Pribat, *Journal of Materials Chemistry A* 2013, 1, 9566; W. McSweeney, H. Geaney, C. O'Dwyer, *Nano Research* 2015, 8, 1395.
- [13] F. Toor, J. B. Miller, L. M. Davidson, W. Duan, M. P. Jura, J. Yim, J. Forziati, M. R. Black, *Nanoscale* 2016, 8, 15448; J. Oh, H.-C. Yuan, H. M. Branz, *Nature Nanotechnology* 2012, 7, 743.
- [14] N. Van Toan, M. Toda, T. Hokama, T. Ono, *Advanced Engineering Materials* 2017, 19, 1700203.
- [15] A. Kristensen, J. K. W. Yang, S. I. Bozhevolnyi, S. Link, P. Nordlander, N. J. Halas, N. A. Mortensen, *Nature Reviews Materials* 2016, 2, 16088; Z. Dong, J. Ho, Y. F. Yu, Y. H. Fu, R. Paniagua-Dominguez, S. Wang, A. I. Kuznetsov, J. K. W. Yang, *Nano Letters* 2017, 17, 7620.
- [16] C. Chang, A. Sakdinawat, *Nat Commun* 2014, 5.
- [17] L. Romano, M. Kagias, K. Jefimovs, M. Stampanoni, *RSC Advances* 2016, 6, 16025.
- [18] L. Li, C. Tuan, C. Zhang, Y. Chen, G. Lian, C. Wong, *Journal of Microelectromechanical Systems* 2018, 1.
- [19] C. V. Thompson, *Annual Review of Materials Research* 2012, 42, 399.
- [20] S. Strobel, C. Kirkendall, J. B. Chang, K. K. Berggren, *Nanotechnology* 2010, 21, 505301.
- [21] S. M. Goodnick, M. Fathipour, D. L. Ellsworth, C. W. Wilmsen, *Journal of Vacuum Science and Technology* 1981, 18, 949.
- [22] L. Romano, M. Kagias, J. Vila-Comamala, K. Jefimovs, L.-T. Tseng, V. A. Guzenko, M. Stampanoni, *Nanoscale Horizons* 2020, 5, 869.
- [23] C. Chartier, S. Bastide, C. Lévy-Clément, *Electrochimica Acta* 2008, 53, 5509.
- [24] C. Chiappini, in *Handbook of Porous Silicon*, (Ed: L. Canham), Springer International Publishing, Cham 2017, 1.
- [25] O. J. Hildreth, W. Lin, C. P. Wong, *ACS Nano* 2009, 3, 4033.
- [26] L. Romano, J. Vila-Comamala, K. Jefimovs, M. Stampanoni, *Microelectronic Engineering* 2017, 177, 59.
- [27] Y. Kim, A. Tsao, D. H. Lee, R. Maboudian, *Journal of Materials Chemistry C* 2013, 1, 220.
- [28] R. Liu, F. Zhang, C. Con, B. Cui, B. Sun, *Nanoscale Research Letters* 2013, 8, 155.
- [29] W. Chern, K. Hsu, I. S. Chun, B. P. d. Azeredo, N. Ahmed, K.-H. Kim, J.-m. Zuo, N. Fang, P. Ferreira, X. Li, *Nano Letters* 2010, 10, 1582.
- [30] J. Kim, H. Han, Y. H. Kim, S.-H. Choi, J.-C. Kim, W. Lee, *ACS Nano* 2011, 5, 3222; C. Q. Lai, H. Cheng, W. K. Choi, C. V. Thompson, *The Journal of Physical Chemistry C* 2013, 117, 20802.

- [31] L. Li, Y. Liu, X. Zhao, Z. Lin, C.-P. Wong, *ACS Applied Materials & Interfaces* 2014, 6, 575.
- [32] N. Franco, J. E. Klepeis, C. Bostedt, T. Van Buuren, C. Heske, O. Pankratov, T. A. Callcott, D. L. Ederer, L. J. Terminello, *Physical Review B* 2003, 68, 045116.
- [33] M. Takahashi, T. Fukushima, Y. Seino, W.-B. Kim, K. Imamura, H. Kobayashi, *Journal of The Electrochemical Society* 2013, 160, H443.
- [34] K. W. Kolasinski, *Nanoscale Research Letters* 2014, 9, 432.
- [35] L. Li, G. Zhang, C. P. Wong, *IEEE Transactions on Components, Packaging and Manufacturing Technology* 2015, 5, 1039.
- [36] P. C. Andricacos, C. Uzoh, J. O. Dukovic, J. Horkans, H. Deligianni, *IBM Journal of Research and Development* 1998, 42, 567.
- [37] C. David, J. Bruder, T. Rohbeck, C. Grünzweig, C. Kottler, A. Diaz, O. Bunk, F. Pfeiffer, *Microelectronic Engineering* 2007, 84, 1172.
- [38] M. Kagias, Z. Wang, V. A. Guzenko, C. David, M. Stampanoni, K. Jefimovs, *Materials Science in Semiconductor Processing* 2019, 92, 73.
- [39] H. Miao, A. A. Gomella, N. Chedid, L. Chen, H. Wen, *Nano Letters* 2014, 14, 3453.
- [40] T.-E. Song, S. Lee, H. Han, S. Jung, S.-H. Kim, M. J. Kim, S. W. Lee, C. W. Ahn, *Journal of Vacuum Science & Technology A* 2019, 37, 030903.
- [41] D. Josell, S. Ambrozik, M. E. Williams, A. E. Hollowell, C. Arrington, S. Muramoto, T. P. Moffat, *Journal of The Electrochemical Society* 2019, 166, D898.
- [42] A. Momose, S. Kawamoto, I. Koyama, Y. Hamaishi, K. Takai, Y. Suzuki, *Japanese Journal of Applied Physics* 2003, 42, L866.
- [43] F. Pfeiffer, M. Bech, O. Bunk, P. Kraft, E. F. Eikenberry, C. Brönnimann, C. Grünzweig, C. David, *Nature Materials* 2008, 7, 134.
- [44] C. Arboleda, Z. Wang, T. Koehler, G. Martens, U. Van Stevendaal, M. Bartels, P. Villanueva-Perez, E. Roessl, M. Stampanoni, *Opt. Express* 2017, 25, 6349.
- [45] M. Kagias, Z. Wang, M. E. Birckbak, E. Lauridsen, M. Abis, G. Lovric, K. Jefimovs, M. Stampanoni, *Nature Communications* 2019, 10, 5130.
- [46] K. Jefimovs, L. Romano, J. Vila-Comamala, M. E. Kagias, Z. Wang, L. Wang, C. Dais, H. Solak, M. Stampanoni, "High-aspect ratio silicon structures by displacement Talbot lithography and Bosch etching", presented at *Advances in Patterning Materials and Processes XXXIV (March 27, 2017)*, San Jose, California, United States, 2017; L. Romano, J. Vila-Comamala, M. Kagias, K. Vogelsang, H. Schiff, M. Stampanoni, K. Jefimovs, *Microelectronic Engineering* 2017, 176, 6; L. Romano, J. Vila-Comamala, H. Schiff, M. Stampanoni, K. Jefimovs, *Journal of Vacuum Science & Technology B, Nanotechnology and Microelectronics: Materials, Processing, Measurement, and Phenomena* 2017, 35, 06G302.
- [47] T. Weitkamp, A. Diaz, C. David, F. Pfeiffer, M. Stampanoni, P. Cloetens, E. Ziegler, *Opt. Express* 2005, 13, 6296.
- [48] T. Donath, M. Chabior, F. Pfeiffer, O. Bunk, E. Reznikova, J. Mohr, E. Hempel, S. Popescu, M. Hoheisel, M. Schuster, J. Baumann, C. David, *Journal of Applied Physics* 2009, 106, 054703.
- [49] A. Yan, X. Wu, H. Liu, *Opt. Express* 2016, 24, 15927.